Molecular structure, mechanical behavior and failure mechanism of the C-terminal cross-link domain in type I collagen

Sebastien G.M. Uzel*,**, Markus J. Buehler*,***,†

* *Laboratory for Atomistic and Molecular Mechanics, Department of Civil and Environmental Engineering, Massachusetts Institute of Technology, 77 Massachusetts Ave. Room 1-235A&B, Cambridge, MA, USA*

** *Department of Mechanical Engineering, Massachusetts Institute of Technology, 77 Massachusetts Ave., Cambridge, MA, USA*

*** *Center for Computational Engineering, Massachusetts Institute of Technology, 77 Massachusetts Ave., Cambridge, MA, USA*

† *Corresponding author, electronic address: mbuehler@MIT.EDU, Phone: +1-617-452-2750, Fax: +1-617-324-4014*

ABSTRACT: Collagen is a key constituent in structural materials found in biology, including bone, tendon, skin and blood vessels. Here we report a first molecular level model of an entire overlap region of a C-terminal cross-linked type I collagen assembly and carry out a nanomechanical characterization based on large-scale molecular dynamics simulation in explicit water solvent. Our results show that the deformation mechanism and strength of the structure is greatly affected by the presence of the cross-link, and by the specific loading condition of how the stretching is applied. We find that the presence of a cross-link results in greater strength during deformation as complete intermolecular slip is prevented, and thereby particularly affects larger deformation levels. Conversely, the lack of a cross-link results in the onset of intermolecular sliding during deformation and as a result an overall weaker structure. Through a detailed analysis of the distribution of deformation by calculating the molecular strain we show that the location of largest strains does not occur around the covalent bonding region, but is

found in regions further away from this location. The insight developed from understanding collagenous materials from a fundamental molecular level upwards could play a role in advancing our understanding of physiological and disease states of connective tissues, and also enable the development of new scaffolding material for applications in regenerative medicine and biologically inspired materials.

1. Introduction

Cross-linking of molecules, fibrils and fibers is a critical feature in numerous connective tissues such as bone, tendon, cartilage or blood vessels [1-3]. In these tissues, the mechanical strength is primarily provided by strong and elastic molecules such as collagen and elastin [4, 5], which arrange into highly organized hierarchical structures [1-3, 6] where the formation of intermolecular covalent cross-links is important in enhancing the mechanical stability of the resulting tissues. However, when the cross-link density increases, as found in elderly individuals, effects such as skin wrinkling, cartilage impairment or bone embrittlement as in osteoporosis and diabetes can occur [7, 8]. This illustrates the role of cross-links in the alteration of material properties in disease states, which eventually leads to a breakdown of key material components of biological systems [5]. The effects of increased cross-link density on increasing the level of brittleness of collagenous tissues was confirmed by earlier coarse-grained computational simulations [9], which investigated the influence of the cross-link density on the strength and the failure mechanism of a two-dimensional bead-spring representation of a collagen microfibril [10]. This study [9] showed that the increase in cross-link density results in a severely altered mechanical behavior, leading to stronger but more brittle collagen fibrils. This altered mechanical response could have important effects on tissue viability. However, a molecular level

understanding of the nanomechanical behavior of cross-linking in collagen fibrils has remained elusive, partly due to the lack of appropriate molecular models with atomistic resolution that would have enabled a systematic analysis. Here we report a study that overcomes this limitation, by developing first a molecular model of a cross-link in a model fibril of type I collagen, and then by applying the model to probe the deformation mechanisms under mechanical loading.

Our study focuses on type I collagen, a fibrous type of collagen and the most abundant of all collagen types in our body. Collagen is defined as a coiled-coil trimer molecule, each of which is composed of the repeated sequence of amino acids Gly-X-Y, where X and Y are commonly found to be proline and hydroxyproline amino acids, respectively. In type I collagen, these tropocollagen molecules self-assemble into pentameric right-handed twisted microfibrils [11] in a staggered fashion, with an axial periodicity of approximately 67 nm [12]. These microfibrils further arrange into fibers that can reach a diameter of several hundreds of nanometers. The structures are stabilized through intermolecular cross-links, formed between telopeptides and adjacent triple helical chains through lysine-lysine covalent bonding [13-15]. Telopeptides, present at both N- and C-termini, are non-helical domains that remain after the cleavage of propeptides [16]. The formation of these cross-links is mediated by the enzyme lysine oxydase [17]. Using x-ray diffraction on rat-tail tendon collagen fibrils, it was recently shown that the C-terminal cross-link occur between lysine 17 and lysine 87 in adjacent molecules, and more importantly, it was suggested that the telopeptide takes a folded configuration as shown in the schematic in Fig. 1 [18]. By utilizing these experimental advances as a guide, we build a full atomistic model of the entire overlap region of two collagen molecules, incorporating a covalent cross-link between the above mentioned lysine residues. Our objective is to generate a simple model system that provides generic insight into the deformation mechanisms and associated mechanical behavior of cross-linked collagen fibrils, for which a high level of control about the underlying genetic sequence and structural arrangement is possible in our *in silico* approach.

2. Materials and Methods

2.1 Molecular structure

To enable a high level of control over the genetic sequence, the triple helical collagen domains are created using the software THeBuScr [19] by inputting the following sequences (these sequences are part of the complete sequence of type I collagen from GenBank RefSeq NM_000088.3 and NM_000089.3 that can be found in www.le.ac.uk/ge/collagen/COL1A1_numbering.pdf and www.le.ac.uk/ge/collagen/COL1A2_numbering.pdf). For the α_1 chains in the C-terminus region:

GARGPAGPQGPRGDKGETGEQGDRGIKGHRGFSGLQGPPGPPGSPGEQGPSGASGPAGPRGPPGSAGAPGKDGLNGLPGPIGPPGPRGRTGDAGPVGPPGPPGPPGPP. For the α_2 chain in the C-terminus region:

GPSGPQGIRGDKGEPGEKGPRGLPGLKGHNGLQGLPGIAGHHGDQGAPGSVGPAGPRGPAGPSGPAGKDGRTGHPGTVGPAGIRGPQGHQGPAGPPGPPGPPGPPGVSGGG. For the α_1 chains in the N-terminus region:

GPMGPSGPRGLPGPPGAPGPQGFQGPPGEPGEPGASGPMGPRGPPGPPGKNGDDGEAGKPGRPGERGPPGPQGARGLPGTAGLPGM**K**GHRGFSGLDGAKGDAGPAGPKGEPGSPGENGAPGQMGPR. For the α_2 chain in the N-terminus region:

GPMGLMGPRGPPGAAGAPGPQGFQGPAGEPGEPGQTGPAGARGPAGPPGKAGEDGHPGKPGRPGERGVVGPQGARGFPGTPGLPGFKGIRGHNGLDGLKGQPGAPGVKGEPGAPGENGTPGQTGAR.

In the collagen sequence pattern G-X-Y, each proline in the Y position is substituted by a hydroxyproline. However, because the force field used here does not account for hydroxylysine, no post-translation modification was considered for the lysines. The C-telopeptides are generated with the Nanoengineer program (http://nanoengineer-1.com). The following sequences are used: SAGFDFSFLPQPPQE**K**AHDGGRYYRA for the α_1 chains, YDFGYDGDFYRA for the α_2 chain.

The three telopeptide segments are attached to the C-terminus region by concatenating both structure files (Protein Data Base [PDB] format). Then, they are positioned in space by manual manipulation using Visual Molecular Dynamics (VMD) [20] in order to reach an approximate alignment with the C-terminus region. In the same fashion, the N-terminus region is juxtaposed

to the C-terminus region in order to achieve an overlap of 30 nm, according to experimental data [18]. Consequently, the telopeptides are shaped so as to reach the particular pattern suggested in [18] as displayed in Fig. 1. This process involves successive displacements of carbon atoms from the backbone toward their final position using VMD and minimization simulations while fixing these atoms. The crosslink is modeled by creating a covalent bond between the two lysine marked by a bold underlined "**K**" in the sequences given above, for one of each α_1 chains in both C- and N-terminus regions. A first step consisted in removing the amino group together with a hydrogen atom connected to the C_ε from one lysine, and all three hydrogen atoms in the amino group from the other lysine. Then, a covalent bond was manually added in the corresponding molecular structure file (PSF file) in order to represent the chemistry of a lysine-lysine cross-link [17].

2.2 Molecular modeling

A first minimization and equilibration is carried out in vacuum to allow the structure to come to a close aggregate. The polypeptide is then solvated in a periodic water box composed of TIP3 water molecules, of dimensions 630 Å $\times$ 55 Å $\times$ 55 Å, leading to a system that includes approximately 175,000 atoms in total (including collagen and water). To model the confinement due to the surrounding collagen molecules that are present in a complete fibril, the walls of the water box are kept fixed at a distance of 10 Å. Finally, the system is subjected to a complete equilibration in order to reach a relaxed state as shown in the Root Mean Square Displacement (RMSD) curve depicted in Fig. 3. The final configuration of the molecule is shown in Fig. 1. In Figs. 1(b) and (c) the entire system investigated here is shown, in full-atom sphere-based and backbone licorice graphical representations, respectively. Fig. 1(d) is a zoomed illustration of the cross-linked region and panel (e) is a detailed representation of the cross-linked lysine residies.

Molecular dynamics simulations are carried out using the NAno Molecular Dynamics (NAMD) code and the Chemistry at HARvard Molecular Mechanics (CHARMM) force field [21, 22] that includes parameters for hydroxyproline amino acids. The electrostatic interactions are modeled by the particle-mesh Ewald summation (PME) method. Energy minimization is performed using a conjugate gradient (CG) scheme. Equilibration runs are carried out at a temperature of 310 K

(= 37 °C). Stretching of the proteins is performed via the steered molecular dynamics (SMD) simulation protocol [23]. This method is based on the concept of pulling the center of mass of a collection of chosen atoms via a spring along the direction of the molecular axis, while keeping the center of mass of another group of atoms fixed through a stiffer spring. Here, the spring constants are $k_{steered} = 3 \times 10^5$ kJ mol^{-1} nm^{-2} and $k_{fixed} = 4 \times 10^3$ kJ mol^{-1} nm^{-2}. In all cases the pulling velocity is set to 1 m·s^{-1}. It was shown that below that pulling velocity the molecular mechanical properties reach an asymptotic regime and do not depend on the pulling speed below this threshold [24]. The atomistic level geometry of the cross-linked structure in PDB format is available upon request.

2.3 Nanomechanical analysis

Four different loading conditions are tested to investigate the behavior of the cross-linked collagen structure, as depicted in Fig. 2. In each set-up, the first four residues in the three strands in the C-terminus region are kept fixed during the SMD simulations (part in the red rectangle in Fig. 2). For the first case ① (the control case) the center of mass of the C$_\alpha$ atoms of the rightmost residues of the N-terminal region is pulled, while the cross-link has been removed. The second case ② corresponds to the same loading condition as the control test, but under the presence of a cross-link. The third ③ and fourth ④ cases correspond to the situation where the load is applied to one strand only, the strand containing the cross-link and one of the strands that does not contain the cross-link, respectively. See also Table 1 for an overview.

2.4 Local strain measurement

The local deformation in each strand within the molecular structure is computed as follows. After applying a moving average to the positions of the C$_\alpha$ atoms in each glycine residue in the helical domains (data extracted from the trajectories), the strain in individual strands is calculated as the relative elongation of these C$_\alpha$ atoms with respect to their initial configuration. The results are reported with a color code ranging from -30 % (white), 0 % (yellow) towards 50 % strain (red-black). For clarity, each strand is drawn separately from its adjacent neighbors and only the real axial positions are represented in this visualization.

In order to identify where the maximum strain is located in each of the chain we calculate the strain in each bond withstanding stress, that is, bonds between N, C_α and C atoms in the backbone, as well as connected atoms in the lysine-lysine cross-link. The location of the maximum strain at a particular time point is identified by a color/marker code. In that representation, chains A, B and C (D, E and F) correspond to the α_1 chain containing the cross-link, the α_1 chain that does not contain the cross-link and the α_2 chain respectively in the C-terminal chain (in the N-terminal chain). If the maximum strain is located in the lysine-lysine cross-link, it is then referred to as "cross-link".

3. Results

Our first observation is that the folded configuration is stable, according to the converging RMSD after 3 ns as depicted in Fig 3. This result suggests that the structure predicted by earlier x-ray diffraction [18] is indeed stable in our model, and provides a validation of the hypothesized geometry of the C-terminal telopeptides.

Fig. 4 shows the mechanical response of the structure by illustrating the force-elongation relationship under the four different loading conditions studied here. In the graph plotted in Fig. 4(a), we observe that the type of loading condition greatly affect that overall mechanical behavior, and in particular after a axial displacement of 50 Å. Below that value, the mechanical responses of all cases considered are similar, which suggests that the influence of cross-links at small deformation is relatively minor, in agreement with previous results [9].

Past the elongation of 50 Å, discrepancies between the various cases considered emerge. Not only does the presence of cross-links affect the response to stretching, but so does the type of loading. Indeed, when comparing cases ① with cases ② or ③, it appears that the presence of a cross-link is responsible for a significant increase in the capacity of the structure to withstand high forces before failure. We note that in cases ② and ③, the intermediate plateau regime corresponds to the unrolling of the telopeptide containing the cross-link, which is critical as it participates in dissipating energy before even stretching the cross-linked domain. However,

curves ① and ④ illustrate the exact same behavior, even though the molecular rearrangement as stretching occurs is different (see final geometries in Fig. 6). Loading case ② seems to be somewhat of a combination of the two limiting cases ③ and ④, as it features a combination of an increase of strength after the plateau region, followed by some yielding that is likely due to the initiation of interstrand delamination as observed in case ④.

To quantify how the strain develops as stretching builds up, a measure of the local strain is computed. After 18 ns of stretching (which corresponds to an elongation of approximately 180 Å), in the presence of a cross-link, the strain is counter intuitively higher in the leftmost region (to the left of the overlap region) than in the cross-link area (Fig. 5). We believe that the chains surrounding the cross-link in the overlap region offer support to the cross-link, therefore shifting the maximum deformation from the triple helix to the gap region. This analysis enables us also to explain the similarities and discrepancies observed in the force-extension graphs. Indeed, cases ① and ④, and similarly cases ② and ③, can be paired up based on their similarities in local deformation patterns.

Finally, Fig. 7 illustrates at which bond the maximum deformation (over the entire fibril) is located as a function of time. This plot first reveals that at small deformation, there is no single bond that withstands the maximum strain consistently. However, as the C-telopeptide containing the cross-link is being unraveled (which corresponds to the onset of the plateau on the force graph), the maximum local strain is located in the cross-link area itself. Then, as the total strain increases, the maximum deformation shifts to the strand that is being pulled on. The graph also suggests that, if failure is defined as a critical bond-level strain reaching a particular threshold, breaking would occur either in the cross-link when unraveling, in the load-bearing chain at large deformation in case ③, or not at all in case ④ (it is expected that failure would occur through delamination of the N-terminal helix).

4. Discussion and conclusion

We have developed a first simple molecular model of the cross-link structure in type I collagen, and have utilized this model to probe the deformation mechanisms under different cases of

mechanical loading. Our results obtained from molecular simulation have revealed a complex nanomechanical mechanism of unraveling of the cross-linked fibril, where the detailed mechanisms depend on the strain level and the specific boundary conditions (Figs. 5 and 7). Our results demonstrated a severe change in the nanomechanical behavior under the presence of cross-links, resulting in a strengthening at large deformation (Fig. 4). These findings corroborate the notion that cross-links contribute to the mechanical stability of collagenous tissues by enhancing the adhesive strength between collagen molecules at a molecular scale [9].

As briefly discussed in the introduction, cross-links can form at both N- and C-termini. However, for the purpose of this study, we only considered the C-terminal cross-link. The first reason is that very little is known from experiment on the exact geometrical organization of the N-telopeptide. Further, the study presented in this paper aims at understanding the molecular phenomenon underlying the failure mechanism between two molecules. Considering that the cross-link at the N-terminal of the second molecule would form with a third molecule, it is unlikely to have major repercussion on the behavior of the system studied here as it would only influence larger scales. Another limitation of our study is that even though telopeptides can contain up to two covalent cross-links, we studied the influence of one cross-link only. We believe that the presence of a second cross-link would not drastically change the overall responses reported here. It would simply change the relative contribution of cases ③ and ④ in the general three-strand loading type. The considerations of these issues are left to future work.

In order to model the behavior at the cross-link as a constitutive model, we develop a simple rheological model based on three simple elements as shown in Fig. 8. The first element accounts for the elastic regime and is represented by an elastic spring; the second is a frictional element, used to model a perfectly plastic material. Finally, the third element that we call the "delay" element was created to account for the delayed response due to the unraveling of the telopeptide. When these blocks are arranged as shown in Fig. 8, the model reproduces the three consecutive regimes predicted by our MD simulations. This model achieves three goals: First, the model offers a simple way to visualize the emergence of successive mechanisms at different levels of deformation. Second, the model could be use to test the sensitivity to the frictional threshold or the length of the "delay" in terms of the overall force-deformation behavior of the fibril. Finally,

we believe that this simple representation is universal to many other cross-links in protein materials that are likely to exhibit the same mechanical response as the one reported here.

Our study suggests that in the presence of a mutation that prevents the cross-link to form (for example, mutations that could occur in diseases such as *osteogenesis imperfecta* [25, 26]) it would have tremendous impact on the mechanical behavior of the fibrillar assembly. Indeed, in such a situation, the absence of cross-link would be generalized to the whole tissue, multiplying the effects reported above by as many tropocollagen molecules as the tissue contains, and could lead to catastrophic failure as reported in previous work [27]. The insight developed from understanding collagenous materials from a fundamental molecular and nanomechanical level upwards is wide-ranging, and could also play a role in advancing the development of scaffolding material for applications in regenerative medicine [28] and other biologically inspired materials.

This work was based on a rather simple model system of only two molecules. This allows us to maintain a simple geometry and thus a certain universality in the behavior of such a cross-linked assembly. In other words, it can be expected that a general overlap of two collagen molecules, cross-linked at one of the telopeptide regions, would have a similar force/extension response as the one depicted here. Future work could focus on building a cross-linked structure based on the low-resolution C_α-trace obtained via x-ray diffraction (e.g. based on the work by Orgel, Hess *et al*. [11]) coupled with protein structure prediction methods such as the Rosetta method [29]. This approach could result in a full three-dimension representation of cross-linked collagen fibrils and provide a powerful platform to build up a bottom-up mechanistic understanding of the mechanical properties of collagenous tissues; albeit the analysis of the mechanisms of deformation with a model would be far more complex. It could also be interesting to investigate the behavior at the N-terminal and couple it with the one reported here. Finally, it would be valuable to construct a full-atomistic three-dimensional micro-fibril model containing both N- and C- terminal cross-links. Further, the results presented here can also bee seen as a challenge to experimental efforts, where a systematic investigation of collagen nanofibrils with and without cross-links, perhaps using optical tweezers or Atomic Force Microscopy experiments [30-32], could complement the molecular simulation studies put forth here.

There are other types of cross-links that appear in collagen fibrils, in addition to the one considered in the present study. Specifically, non-enzymatic cross-links known as Advanced Glycation End-products (AGE) cross-links are another form of cross-links found in collagens. These cross-links are also thought to be involved in the alteration of the mechanical properties of collagenous tissues. The only type of AGE cross-link that would likely affect the mechanical behavior of the fibrils or fibers is glucosepane, an arginine-lysine glycated cross-link whose concentration, in aging or diabetic tissue, could reach values high enough not to be neglected. This type of cross-link has not been considered in this study for the following reasons. First, little is known about the formation pathways and exact locations of theses cross-links. Also, recent studies suggested that the glycated cross-links are likely to be present in the triple helical domains of adjacent molecules, remote from the region of interest of our study. Finally, these cross-links become prominent in aging or pathologic tissues, which are not in the scope of this manuscript. As more data become more available on this matter, it would indeed be interesting to see how this other family of cross-link contributes to mechanical breakdown in aging and/or diabetic tissues.

Finally, the state of hydration can have tremendous effects on the mechanical behavior of a collagen assembly at multiple levels. Because we focused on the behavior on a single pair of molecules in this study, we did not vary the hydration state and rather, let the molecules equilibrate in a large explicit water box filled with a large amount of surrounding water. Variations of the water content will become an issue, however, when we investigate the response of a full atomistic/cross-linked (three-dimensional) collagen micro-fibril as briefly outlined above. With such a model we would be able to vary the water content and examine its influence on the stiffness, strength and other mechanical parameters of the collagen fibril. This is left to future work.

References

1.   Gelse, K., E. Poschl, and T. Aigner, *Collagens - structure, function, and biosynthesis.* Advanced Drug Delivery Reviews, 2003. **55**(12): p. 1531-1546.

2.   Fratzl, P. and R. Weinkamer, *Nature's hierarchical materials.* Progress in Materials Science, 2007. **52**: p. 1263-1334.

3.   Gupta, H.S., J. Seto, S. Krauss, P. Boesecke, and H.R.C. Screen, *In situ multi-level analysis of viscoelastic deformation mechanisms in tendon collagen.* Journal Of Structural Biology, 2010. **169**(2): p. 183-191.

4.   Alberts, B., A. Johnson, J. Lewis, M. Raff, K. Roberts, and P. Walter, *Molecular Biology of the Cell.* 2002, New York: Taylor & Francis.

5.   Buehler, M.J. and Y.C. Yung, *Deformation and failure of protein materials in physiologically extreme conditions and disease.* Nat Mater, 2009. **8**(3): p. 175-88.

6.   Ortiz, C. and M.C. Boyce, *Materials science - Bioinspired structural materials.* Science, 2008. **319**(5866): p. 1053-1054.

7.   Bailey, A.J., *Molecular mechanisms of ageing in connective tissues.* Mechanisms of Ageing and Development, 2001. **122**(7): p. 735-755.

8.   Saito, M. and K. Marumo, *Collagen cross-links as a determinant of bone quality: a possible explanation for bone fragility in aging, osteoporosis, and diabetes mellitus.* Osteoporos Int, 2009. **21**(2): p. 195-214.

9.   Buehler, M.J., *Nanomechanics of collagen fibrils under varying cross-link densities: Atomistic and continuum studies.* Journal of the Mechanical Behavior of Biomedical Materials, 2008. **1**(1): p. 59-67.

10.   Buehler, M.J., *Nature designs tough collagen: Explaining the nanostructure of collagen fibrils.* P. Natl. Acad. Sci. USA, 2006. **103**(33): p. 12285–12290.

11.   Orgel, J., T.C. Irving, A. Miller, and T.J. Wess, *Microfibrillar structure of type I collagen in situ.* Proceedings of the National Academy of Sciences of the United States of America, 2006. **103**(24): p. 9001-9005.

12.   Piez, K.A. and B.L. Trus, *A New Model for Packing of Type-I Collagen Molecules in the Native Fibril.* Bioscience Reports, 1981. **1**(10): p. 801-810.

13.   Reiser, K., R.J. McCormick, and R.B. Rucker, *ENZYMATIC AND NONENZYMATIC CROSS-LINKING OF COLLAGEN AND ELASTIN.* Faseb Journal, 1992. **6**(7): p. 2439-2449.

14.   Knott, L. and A.J. Bailey, *Collagen cross-links in mineralizing tissues: A review of their chemistry, function, and clinical relevance.* Bone, 1998. **22**(3): p. 181-187.

15.   Light, N.D. and A.J. Bailey, *CHEMISTRY OF THE COLLAGEN CROSS-LINKS - PURIFICATION AND CHARACTERIZATION OF CROSS-LINKED POLYMERIC PEPTIDE MATERIAL FROM MATURE COLLAGEN CONTAINING UNKNOWN AMINO-ACIDS.* Biochemical Journal, 1980. **185**(2): p. 373-381.

16.   Prockop, D.J. and K.I. Kivirikko, *Collagens - Molecular-Biology, Diseases, and Potentials for Therapy.* Annual Review of Biochemistry, 1995. **64**: p. 403-434.

17.   Eyre, D.R., M.A. Weis, and J.J. Wu, *Advances in collagen cross-link analysis.* Methods, 2008. **45**(1): p. 65-74.

18.   Orgel, J., A. Miller, T.C. Irving, R.F. Fischetti, A.P. Hammersley, and T.J. Wess, *The in situ supermolecular structure of type I collagen.* Structure, 2001. **9**(11): p. 1061-1069.

19.   Rainey, J.K. and M.C. Goh, *An interactive triple-helical collagen builder.* Bioinformatics, 2004. **20**(15): p. 2458-2459.

20.   Humphrey, W., A. Dalke, and K. Schulten, *VMD: Visual molecular dynamics.* Journal Of Molecular Graphics, 1996. **14**(1): p. 33.

21. MacKerell, A.D., D. Bashford, M. Bellott, R.L. Dunbrack, J.D. Evanseck, M.J. Field, S. Fischer, J. Gao, H. Guo, S. Ha, D. Joseph-McCarthy, L. Kuchnir, K. Kuczera, F.T.K. Lau, C. Mattos, S. Michnick, T. Ngo, D.T. Nguyen, B. Prodhom, W.E. Reiher, B. Roux, M. Schlenkrich, J.C. Smith, R. Stote, J. Straub, M. Watanabe, J. Wiorkiewicz-Kuczera, D. Yin, and M. Karplus, *All-atom empirical potential for molecular modeling and dynamics studies of proteins.* Journal Of Physical Chemistry B, 1998. **102**(18): p. 3586-3616.

22. Karplus, M. and J.A. McCammon, *Molecular dynamics simulations of biomolecules.* Nature Structural Biology, 2002. **9**(9): p. 646-652.

23. Lu, H., B. Isralewitz, A. Krammer, V. Vogel, and K. Schulten, *Unfolding of titin immunoglobulin domains by steered molecular dynamics simulation.* Biophysical Journal, 1998. **75**(2): p. 662-671.

24. Gautieri, A., M.J. Buehler, and A. Redaelli, *Deformation rate controls elasticity and unfolding pathway of single tropocollagen molecules.* J Mech Behav Biomed Mater, 2009. **2**(2): p. 130-7.

25. Rauch, F. and F.H. Glorieux, *Osteogenesis imperfecta.* Lancet, 2004. **363**(9418): p. 1377-1385.

26. Sillence, D.O., A. Senn, and D.M. Danks, *GENETIC-HETEROGENEITY IN OSTEOGENESIS IMPERFECTA.* Journal of Medical Genetics, 1979. **16**(2): p. 101-116.

27. Gautieri, A., S. Uzel, S. Vesentini, A. Redaelli, and M.J. Buehler, *Molecular and Mesoscale Mechanisms of Osteogenesis Imperfecta Disease in Collagen Fibrils.* Biophysical Journal, 2009. **97**(3): p. 857-865.

28. Harley, B.A., J.H. Leung, E.C. Silva, and L.J. Gibson, *Mechanical characterization of collagen-glycosaminoglycan scaffolds.* Acta Biomater, 2007. **3**(4): p. 463-74.

29. Das, R. and D. Baker, *Macromolecular modeling with Rosetta.* Annual Review of Biochemistry, 2008. **77**: p. 363-382.

30. Bozec, L. and M. Horton, *Topography and mechanical properties of single molecules of type I collagen using atomic force microscopy.* Biophysical Journal, 2005. **88**(6): p. 4223-4231.

31. Sun, Y.L., Z.P. Luo, A. Fertala, and K.N. An, *Stretching type II collagen with optical tweezers.* Journal Of Biomechanics, 2004. **37**(11): p. 1665-1669.

32. Farre, A., A.V.D. Horst, G.A. Blab, B.P.B. Downing, and N.R. Forde, *Stretching single DNA molecules to demonstrate high-force capabilities of holographic optical tweezers.* Journal of Biophotonics, 2010. 10.1002/jbio.200900107.

Table and table legend

Table 1: Overview of all loading conditions considered here.

Case	Cross-link	Description
①	—	Left end fixed, no cross-link, pull on all three polypeptides
②	✓	Left end fixed, with cross-link, pull on all three polypeptides
③	✓	Left end fixed, with cross-link, pull on the polypeptide chain that contains the cross-link
④	✓	Left end fixed, with cross-link, pull on the polypeptide chain that does not contain the cross-link
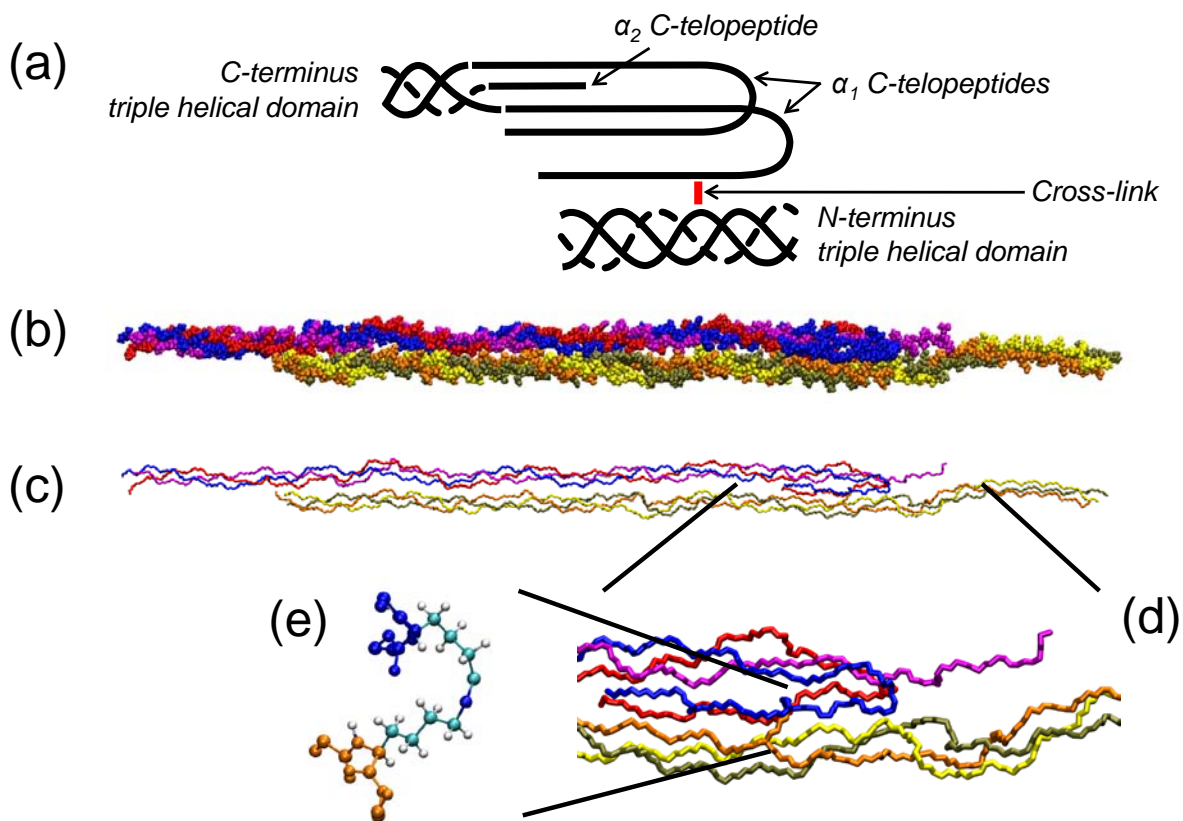
Figure 1: Representations of the cross-linked assembly. Panel (a) shows a schematic of the suggested cross-link structure based on low resolution x-ray diffraction results [18]. Panels (b) and (c) depict the complete equilibrated system as full-atom sphere-based and backbone licorice graphical representations, respectively. Panel (d) is a zoomed-in of panel (c), showing the cross-link region in more detail. Panel (e) presents the detailed chemical structure of the cross-link between both lysine residues (water molecules not shown in the visualizations).
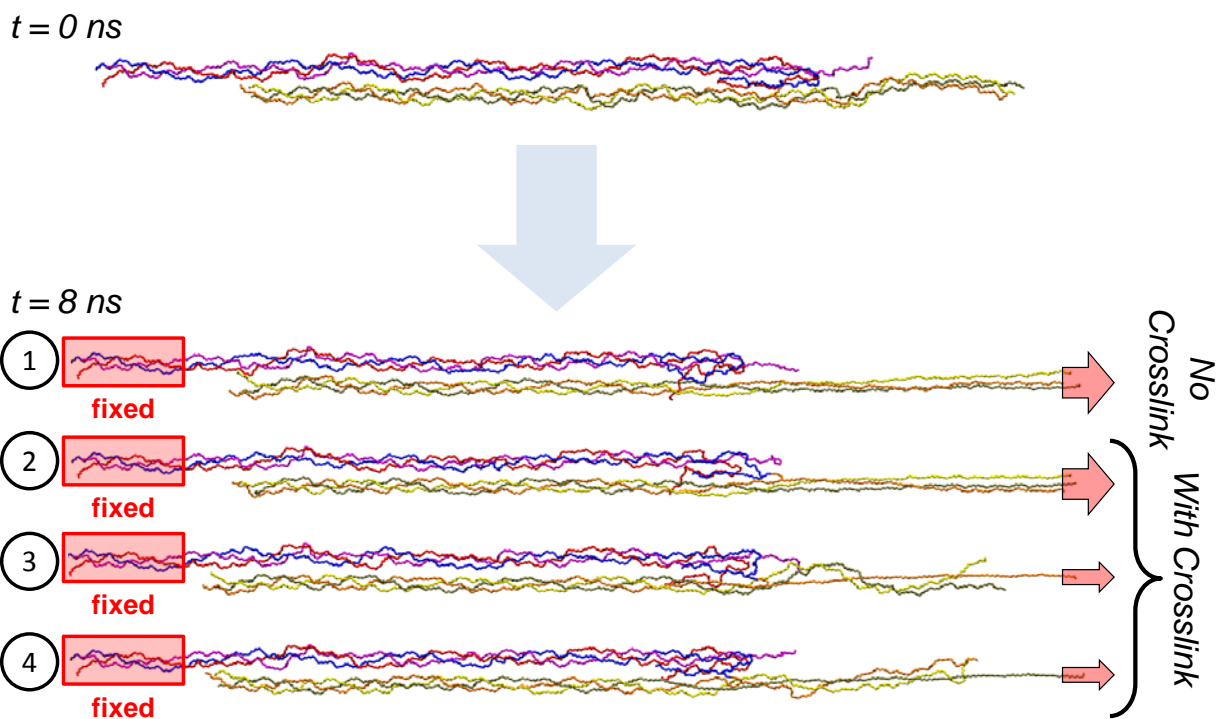
Figure 2: Representation of the loading conditions. In all the set-ups, the 4 leftmost residues in each strand (red rectangle) are kept fixed. In case ①, the crosslink has been removed and the C_α carbons of the rightmost residues in each strand are being stretched. The same loading is applied to case ②, this time in the presence of the crosslink. Case ③ and ④ correspond to the situation where one strand only is being pulled. For case ③, the chain that contains the crosslink is pulled, in case ④, one of the chains that do not contain the crosslink is stretched (see also Table 1).
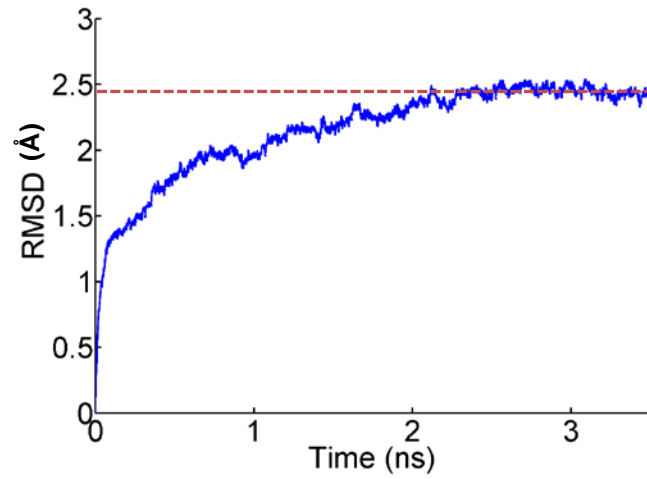
Figure 3: Root Mean Squared Displacement (RMSD) graph of the system, fully solvated in explicit water. This plot shows that the structure has reached an equilibrated (that is, relaxed) state.
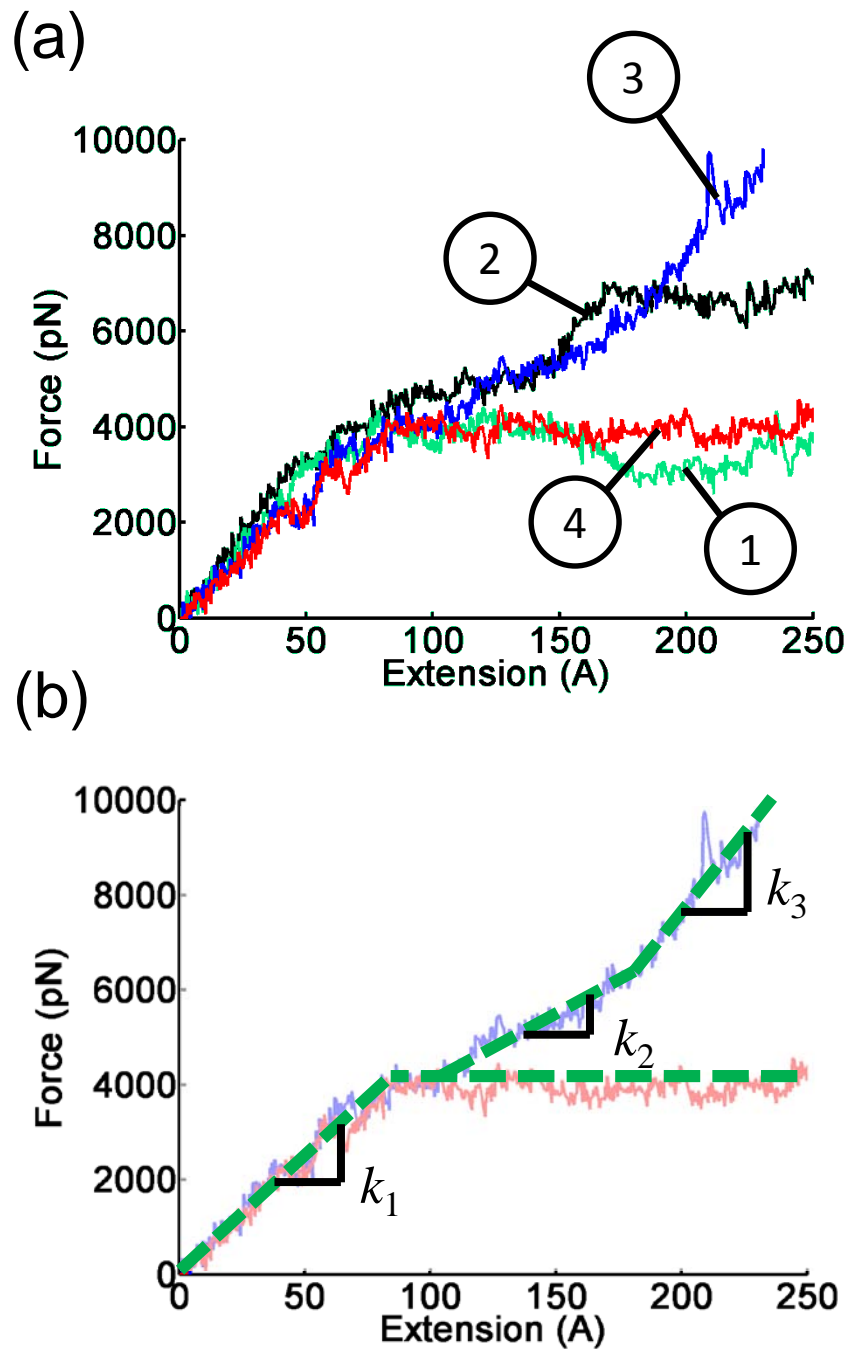
Figure 4: Force-extension curves for the four types of loading considered. In panel (a), the four cases of loading are represented (the numbering is the same as in Fig. 2). In all the cases ①-④, a plateau is reached at approximately 4000 pN, which corresponds to the onset of slip between the C- and N-terminus regions. Panel (b) exhibits the different regimes observed during stretching

for loading conditions ③ and ④ (k_i denote local stiffnesses in the force-extension curve). In regime $k_2 < k_1$, dissipation through slippage and extension due to the stretching of the crosslink occurs. In regime $k_3 > k_1$: stiffening due to the crosslink.
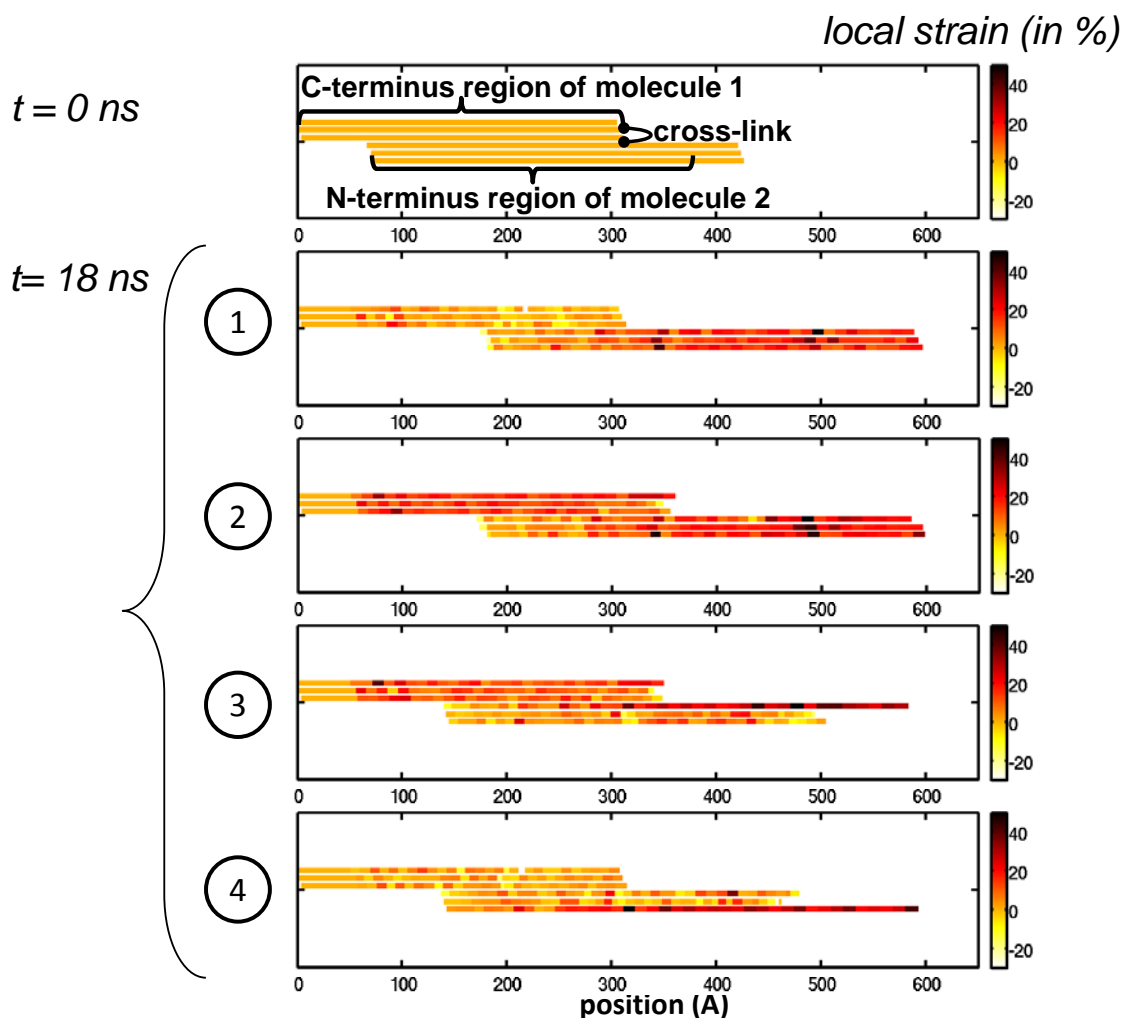
Figure 5: Representation of the strain computed from the position of the C_α atoms in glycine residues in the triple helical domains. The first row shows the initial configuration, the four following rows correspond to cases ①-④, after 18 ns of stretching. These results reveal that the overlap regions act as a buffer. In case ③, it prevents the stress from concentrating along the strands containing the cross-link. Instead the deformation is transferred to the leftmost, triple helical region. In case ④, the overlap region is the area of energy dissipation and prevents from a complete delamination of the polypeptides.
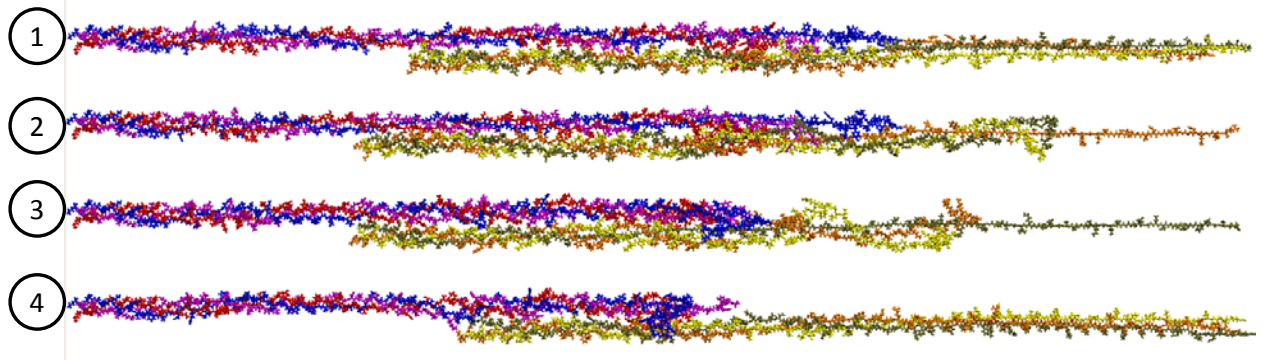
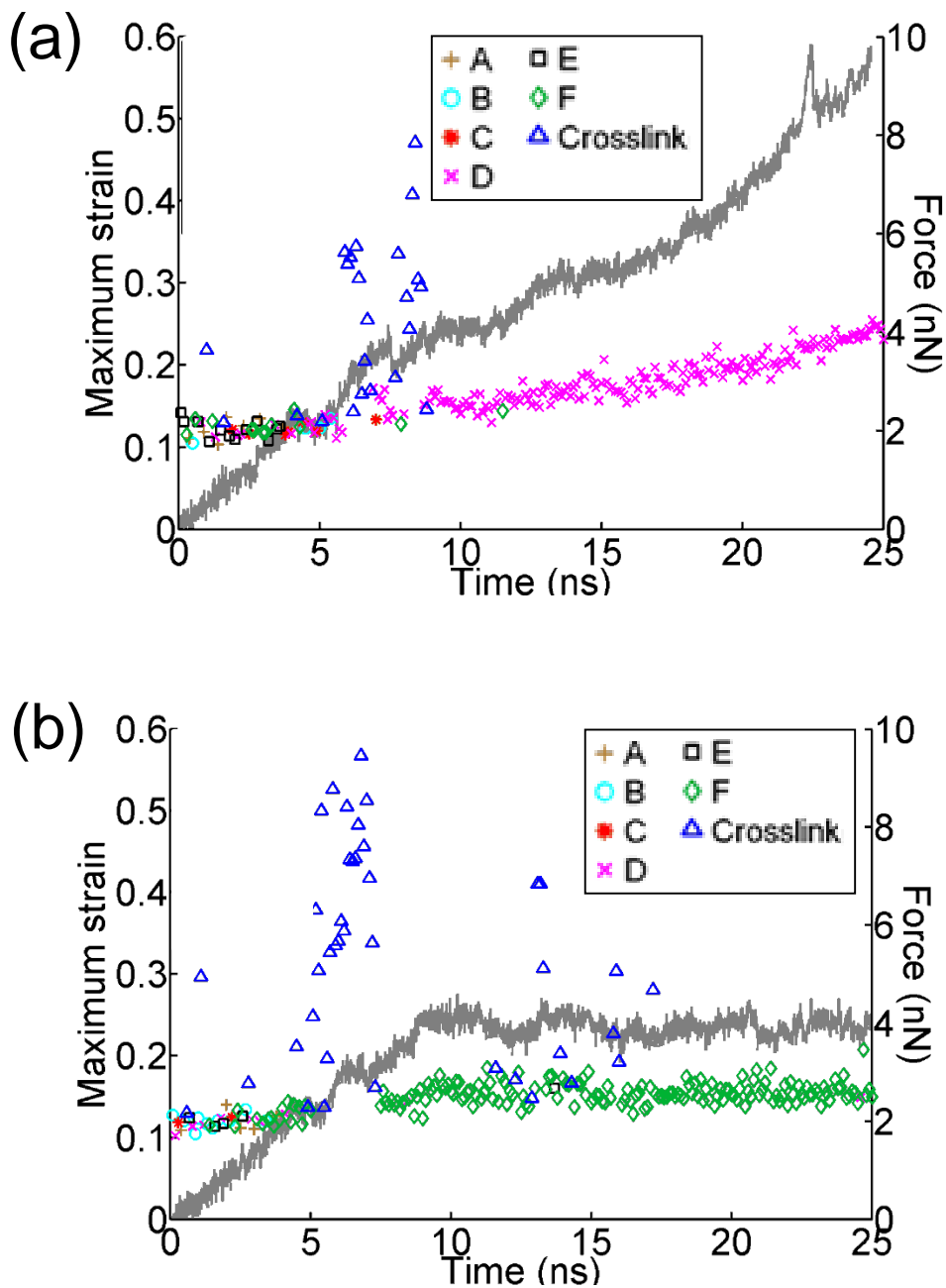**Figure 6**: Structural geometry at large deformation, for all four loading cases considered here.

Figure 7: Maximum bond strain in the backbone of the structure and in the cross-link as a function of time, in loading condition ③ (panel (a)) and ④ (panel (b)). These graphs reveal that as the crosslink is being unraveled (at $t \approx 6\text{-}7$ ns) the maximum strain is located in the cross-link area. However, as the structure is being more a more stretched, this maximum shifts to the strand that withstands the loading.
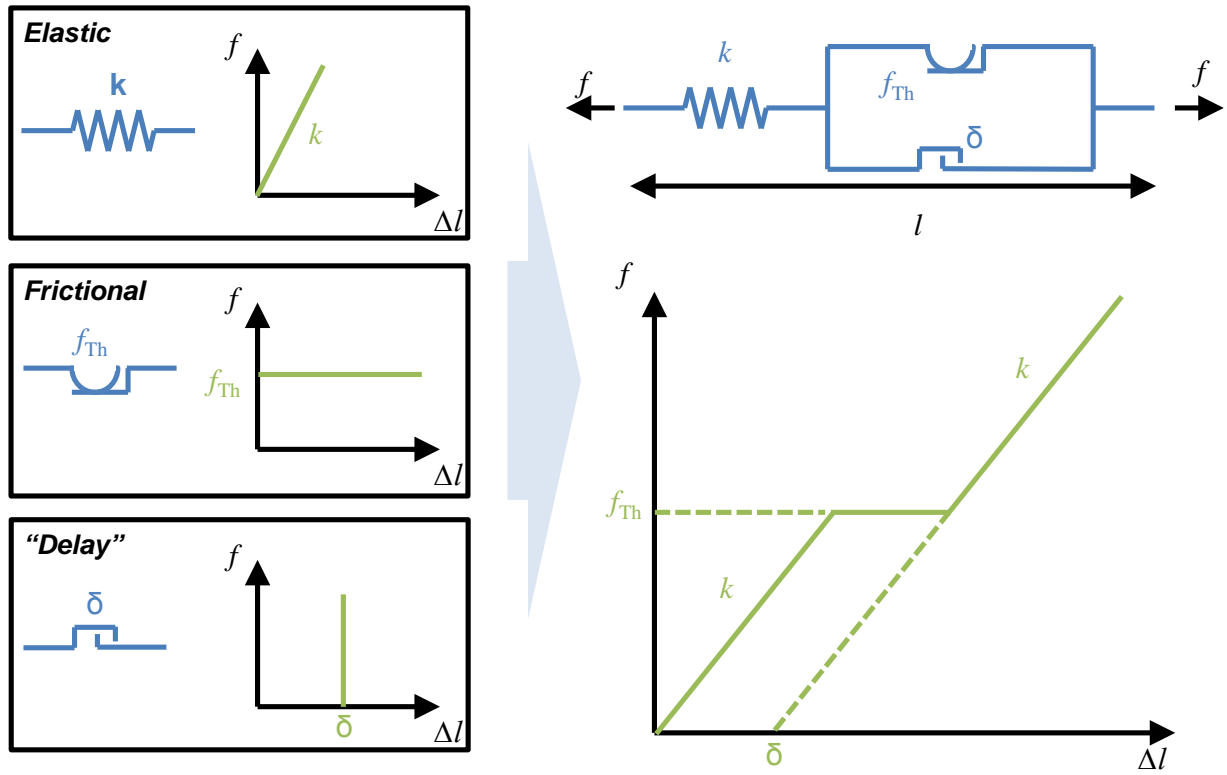
Figure 8: Rheological model accounting for the contribution of the crosslink through the element "delay". The elastic element and the frictional both account for the tensile stiffnesses and the intermolecular slippage respectively.